International Journal of Materials and Chemistry 2012, 2(1): 1-9
DOI: 10.5923/j.ijmc.20120201.01

In Vitro Bioactivity of Collagen/Calcium Phosphate Silicate Composites, Cross-Linked with Chondroitin Sulfate

Lachezar Radev[1,*], Nasser Y. Mostafa[2], Irena Michailova[1], Isabel M. M. Salvado[3], Maria H. V. Fernandes[3]

[1]Department of Fundamental Chemical Technology, University of Chemical Technology and Metallurgy, Sofia, 1756, Bulgaria
[2]ChemistryDepartment, Faculty of Science, Taif University, Taif 888, Kingdom of Saudi Arabia
[3]Department of Silicate Technology, University of Aveiro and CICECO, Aveiro, 3810-193, Portugal

Abstract In this work we present the experimental results on synthesis structure and in vitro bioactivity of collagen (C)/calcium phosphate silicate (CPS)/chondroitin sulfate (ChS) composites with C/CPS ratio of 25:75 wt. % and 75:25wt. %. The synthesized composites were characterized by XRD, FTIR and SEM/EDS. XRD and FTIR before in vitro test proved that the carbonate containing hydroxyapatite (CO_3HA) formed *in situ*. After in vitro test for 3 days in 1.5 SBF, the nucleation of B-type CO_3HA was estimated on the obtained C/CPS=75:25 wt. % composite with cauliflower-like assembly. On the C/CPS=25:75 wt. % amorphous hydroxyapatite (HA) layer was observed.

Keywords Collagen, Calcium Phosphate Silicate, *in Vitro* Bioactivity, Chs

1. Introduction

It should be remembered that proteoglycans have been implicated in the process of regulation of hydroxyapatite (HA) formation and growth in the process of cartilage calcification. In series of papers S.-H. Rhee and J. Tanaka examined the inhibitory effect of chondroitin sulfate (ChS) on HA growth via regulation by the functional groups (COO^- and $-SO_3^-$) of ChS template[1-3]. On the base of FTIR results they proved that the COO^- and $-SO_3^-$ ions showed the "red shift", i. e. formed the chemical interactions between HA crystals and them during the precipitation process[1-3]. H. Jiang et al. studied the nucleation kinetics of HA and quantified the effect of ChS on HA nucleation[4]. The experimental results obtained demonstrated that ChS can suppress the supersaturation-driven mismatch and promote of a highly ordered HA crystalline assembly[4]. X. Xiao et al. also demonstrated that the concentration of ChS significantly affects the morphology of produced HA/ChS composites[5]. They also proved that the prepared HA in the presence of ChS is carbonate containing hydroxyapatite (CO_3HA)[5]. Others investigated the crystallization behavior of HA/ Collagen (HA/Coll) gels in the presence of ChS under physiological conditions. They concluded that ChSplay an important role in the regulation of biomineralization[6]. S–H. Rhee et al. prepared 80HA/8Coll/12ChS (wt. %) nanocomposite via co-precipitation method from $Ca(OH)_2$, H_3PO_4 solution containing collagen and ChS, respectively[7]. On the base of the obtained results they proved that when short ChS fibres are mixed with long collagen fibres, the short ChS fibres might be bound to the long collagen fibres with the same axis direction. After that HA crystals start to growth on the collagen fibres[7]. M. Chang modified gelatin (Gel) matrix by the introduction of ChS and then he studied the formation of HA/Gel/ChSnanocomposite[8]. He prepared this composite by mixing of $Ca(OH)_2$ with aqueous solution of H_3PO_4, gelatin and ChS, respectively and proved that the incorporation of ChS into the Gel matrix contributed to the increase of the organic/inorganic interaction between HA and organic matrix, composed by Gel and ChS[8].

In our previous works we have synthesized some bioactive calcium phosphate silicate (CPS) ceramics[9-11]. We observed that the prepared ceramics were *in vitro* bioactive for different periods of time. On this base we have prepared *in vitro* bioactive composites with some biodegradable polymers without[12-15] and with[16] cross-linkage.

The purpose of our article is to prepare, characterize and evaluate the *in vitro* bioactivity of collagen/calcium phosphate silicate (C/CPS) composites in the presence of ChS.

2. Experimental Part

Preparation of the composites

The CPS ceramic powder as an inorganic part of the composites obtained has been synthesized via polystep sol-gel method with Ca/P+Si molar ratio 1.89. The composition of the gel obtained was 62.6 wt. % CaO, 26.8 wt. % SiO_2 and 10.6 wt. % P_2O_5. The procedure for the synthesis and evaluation of the structure of the prepared CPS ceramics was described in our previous work[9]. Collagen type I,

* Corresponding author:
l_radev@abv.bg (LachezarRadev)
Published online at http://journal.sapub.org/ijmc

taken in amounts corresponding to the composite content was diluted in 15 ml CH_3COOH for 24 h at room temperature under intensively stirring. The C/CPS composite samples, in two types of proportions 25:75 wt. % and 75:25 wt. % were synthesized by adding CPS powder to the C solution with constant stirring for 6 h. pH of the obtained mixture was equal to 2. After homogenation time, pH was adjusted to 9 using 25% NH_4OH. ChS was added as cross-linking agent in the quantity equal to 5% degree of linkage, calculated on the base of terminated NH_2 groups of collagen. The composite materials obtained were dried at 70°C for 12 h under vacuum.

***In vitro* test for bioactivity**

Bioactivity of the composites obtained was evaluated by examining the apatite formation on their surfaces in 1.5 SBF solutions. The 1.5 SBF was prepared from different reagents as follow: NaCl = 11.9925 g, $NaHCO_3$ = 0.5295 g, KCl = 0.3360 g, $K_2HPO_4.3H_2O$ = 0.3420 g, $MgCl_2.6H_2O$ = 0.4575 g, $CaCl_2.2H_2O$ = 0.5520 g, Na_2SO_4=0.1065 g, and buffering at pH 7.4 at 36.5℃ with 9.0075 g of *tris* (hydroxymethyl) aminomethane (TRIS) and 1M HCl in distilled water. A few drops of 0.5% $NaN_3$was added to the 1.5SBF solution to inhibit the growth of bacteria[17].

The synthesized composites were pressed at 50 MPa with PVA to obtain disc specimens (12 mm diameter and 2 mm thick) and then immersed in 1.5SBF at the human body temperature (36.6℃) in polyethylene bottles in a static condition for 3 days. After soaking the specimens were removed from the fluid, gently rinsed with distilled water, and then dried at 36.6℃ for 12h.

Methods for analysis

The structure and *in vitro* bioactivity of composite materials obtained was monitored by X-ray diffraction (XRD) analysis, Fourier transform infrared (FTIR) spectroscopy and scanning electron microscopy with energy dispersive X-ray spectroscopy (SEM-EDS). Powder XRD spectra were collected within the range from 10 to 80° (2θ) with a constant step 0.04° (2θ) and counting time 1s/step on a Bruker D8 Advance diffractometer with CuKα radiation and SolX detector. The spectra were evaluated with the Diffrac*plus* EVA package. FTIR transmission spectra for the samples obtained were recordered by using of aBruker Tensor 27 spectrometer with a scanner velocity 10kHz. KBr pellets were prepared by mixing ~1 mg of the samples with 300 mg KBr. Transmission spectra were recordered using MCT detector with 64 scans and 1 cm^{-1} resolution. SEM technique was employed to observe the particle-size and agglomeration of the synthesized composites before and after *in vitro* test in 1.5 SBF solution. For this a very small amount of a powder was placed on an adhesive carbon tape, coated with gold for 1 min and then observed in a JEOL SEM (model JSM-35 CF, Japan). Energy dispersive X-ray spectroscopy (EDS) was performed for the chemical microanalysis using EDAX system attached to the SEM. After 3 days of immersion, the samples were taken out from 1.5 SBF and the ion concentrations of Ca, P and Si in the solutions were measured by inductively coupled plasma atomic emission spectroscopy (ICP-AES, IRIS, 1000, Thermo Elemental, USA).

3. Results and Discussionanalysis of the Composites before in *Vitro Test*

XRD data for the prepared C/CPS samples with different quantity of the organic/inorganic components are given in Fig. 1

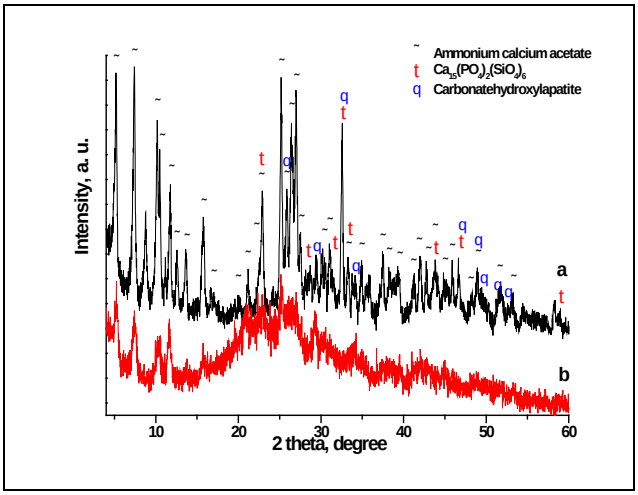

Figure 1. XRD for the C/CPS samples with 25:75 wt. % (a) and 75:25 wt. % (b)

From the depicted Fig. 1 it can be seen that the presence of three crystalline phases ammonium calcium acetate (PDF 22-0026), $Ca_{15}(PO_4)_2(SiO_4)_6$ (PDF 83-1494) and carbonate hydroxyapatite (PDF 19-0272), which is formed *in situ* in the prepared composites, are observed.

FTIR spectra of the synthesized C/CPS samples are shown in Figure 2.

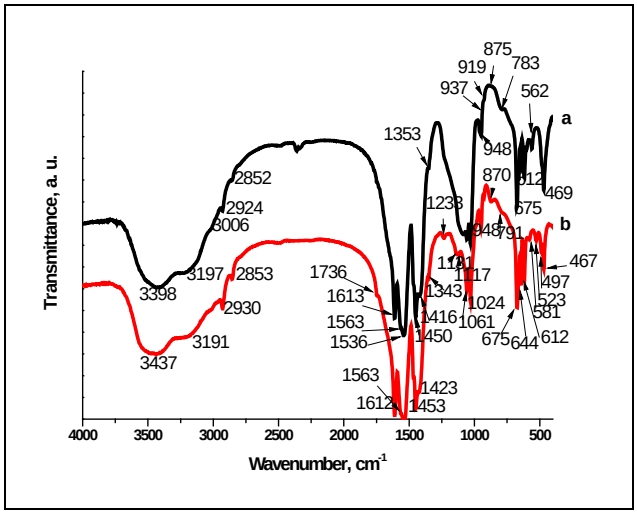

Figure 2. FTIR spectra for the C/CPS composites: 25:75 wt. % (a) and 75:25 wt. % (b)

From the presented FTIR spectra we can observe that they have very complicated character.

The study of the processes of eventual interaction between C and CPS ceramic, the FTIR spectra of pure C and C/CPS

(Fig. 2) were compared.

First of all, in the spectrum of pure collagen (data are not shown here), the amide I peak centered at 1656 cm^{-1} predominantly corresponds to the C=O stretch vibration[12]. From the other studies, the amide I band in a bone spectrum is representative of the collagen content and structure[18]. The amide II, positioned at 1550 cm^{-1} could be ascribed to the presence of N-H plane band and the C-H stretch vibration[18]. For the amide III bands there is a band assigned at 1241 cm^{-1}[19].

As shown in the presented Fig. 3, the amide I band was changed and shifted to lower wavenumbers to 1613 (1612) cm^{-1} for both prepared composites. This change could be assigned to the presence of ChS and to its crucial role into the two composites. In numerous of the articles S.-H. Rhee and J. Tanaka founded that the asymmetrical stretching modes of COO^- and SO_3^- ions in ChS were detected at 1632 cm^{-1} and 1234 cm^{-1}[1-3]. They wrote that after formation of HA crystals in the presence of ChS as a template, these modes were detected at 1613cm^{-1} and 1228 cm^{-1}, respectively. They also concluded that the observed "red shift" caused a chemical interaction between HA crystals and the COO^- and SO_3^- groups of the ChS during the precipitation process. In our case, we assume that observed "red shift" form 1632 cm^{-1} to 1613 (1612) cm^{-1} (Fig. 3, curves a and b) may be due to the chemical interactions between COO^- and Ca^{2+} from the partially dissolved CPS ceramic powders, i. e the bands posited at 1613 (1612) cm^{-1} could be ascribed to the presence of $(COO)_2Ca$.

Furthermore, there is possible and an another interpretation, concerning the presence of the "red shift" form 1656 cm^{-1} (for pure collagen) to 1613 (1612) cm^{-1} for both prepared composites. Alili in him PhD thesis showed, that amide I bands for denaturated and aggregated proteins are posited between 1610 and 1620 cm^{-1}[20]. In the same manner, Liard et al.[21] and Petibois et al.[22] found that the band centered at 1615 cm^{-1} can be assigned to the presence of β-sheet conformation in collagen. On the base of these founding we can assume that collagen undergoes denaturation in the process of preparation of the composites in the presence of CPS ceramic and ChS, which leads to the formation of β-sheet structures.

Therefore, the presence of bands posited at 1613 (1612) cm^{-1} is due to the two processes: (i) chemical interaction between COO^- from ChS and Ca^{2+} from partially dissolved in acetic acid CPS powder, and (ii) denaturation of collagen and formation of β-sheet conformation.

In addition, the partial dissolution of CPS ceramic in the synthesized from us composites can be evaluate from the presence of the bonds (Fig. 3) posited at: 1353 cm^{-1} (curves a and b), which are assigned to the symmetric methyl bending vibrations of the acetate anion; 1416 cm^{-1} for the C/CPC= 25:75 wt. % (curve a) and 1423 cm^{-1} for the C/CPS= 75:25 wt. % (curve b), which present the asymmetric methyl bending for the half-hydrated and monohydrated calcium acetate species, and the presence of an intense bands at 1536 cm^{-1} (for both composites), which may be the result of antisymmetric C-O stretching vibration[23]. In accordance with the same article, the bands at 612 cm^{-1} (curves a and b), 644 cm^{-1} (curve b) and 675 cm^{-1} (curves a and b) could be assigned to the presence of O-C-O fragments[23]. The C-C stretching vibration of the acetate ion has split into a three peaks future, depicted in Fig. 3, at 919 cm^{-1}, 937 cm^{-1} (curve a), 945 cm^{-1} (curve a and b) in the half-hydrated acetates[23]. On the other hand, the band posited at 1024 and 1061 cm^{-1} could be denoted as PO_4^{3-}, Si-O-Si or may be CH_3 groups in the less hydrated acetates[9,23]. Briefly, from the presented FTIR results, we concluded that the presented FTIR data are in accordance to XRD results.

In addition, the presence of a small absorption band at 871 (870) cm^{-1} could be assigned to the HPO_4^{2-} ion in HA structure[24]. In our case, when CPS ceramic powder is added into the acidic collagen solution, some of the particles will dissolve into the CH_3COOH to produce Ca^{2+}, PO_4^{3-} and SiO_4^{4-}. Furthermore, PO_4^{3-} may to give HPO_4^{2-} according to the reaction: $H^+ + PO_4^{3-} \rightarrow HPO_4^{2-}$[25]. The presence of CO_3^{2-} modes, centered at 1353 cm^{-1} (curves a and b), 1416 cm^{-1} (curve a), 1423 cm^{-1} (curve b), 1450 cm^{-1} (curve a) and 1453 cm^{-1} (curve b) indicate that the synthesized composites are similar to the natural bone[26,27]. For the presence of these bonds we can conclude that the Ca-deficient carbonate containing hydroxyapatite (Ca-def. CO_3HA) formed *in situ* under the experimental conditions. The bands, posited at 469 (467) cm^{-1}, 497 cm^{-1} (curve b), 562 cm^{-1} (curve a), 581 cm^{-1} (curve b) and 612 cm^{-1} (curves a and b) can be assigned to the SiO_4^{4-} and PO_4^{3-} groups[28,29].

On the base of FTIR analysis of the prepared C/CPS composites before *in vitro* test we can make the following conclusions:

1. Ca-def. CO_3HA was formed in situ: HPO_4^{2-} ions are present into the samples.

2. Ca^{2+} from partially dissolved CPS ceramic powder may bind with COO^- from ChS and form $(COO)_2Ca$. The collagen undergoes conformation changes due to the formation of β-sheets structures.

3. Calcium acetates also formed in the synthesized composites: the characteristic bands are present.

4. The FTIR data confirmed XRD results.

SEM micrographs of the synthesized C/CPS composites with different quantity of C and CPS are given in Figs. 3 and 4.

Figure 3 presents SEM images of the C/CPS=25:75 wt. % before soaking in 1.5 SBF for 3 days.

As can be seen from the presented images, C/CPS composite with 25:75 wt. % ratio depicts a porous microstructure, similar to the structure of the mineral bone. The pore size ranges from 1 to 7 μm depicts that the synthesized composite is not high porous, because the CPS powder in it is 75 wt. %. In addition the presence of collagen fibrils are also clearly visible on the SEM image. The crystals with a quasi-tubular morphology are also visible. The presence of these crystals could be assigned to the calcium acetates in the composites. From the SEM image at high magnification value (Fig. 3, b) it is also visible that the collagen fibril covered with the

particles in a bright colour with globular morphology. The size ranges of these particles are from 0.1 to 0.5 μm. On the other hand in the presented SEM image is also visible that the in situ formed Ca- def. CO_3HA has a brittle-like morphology.

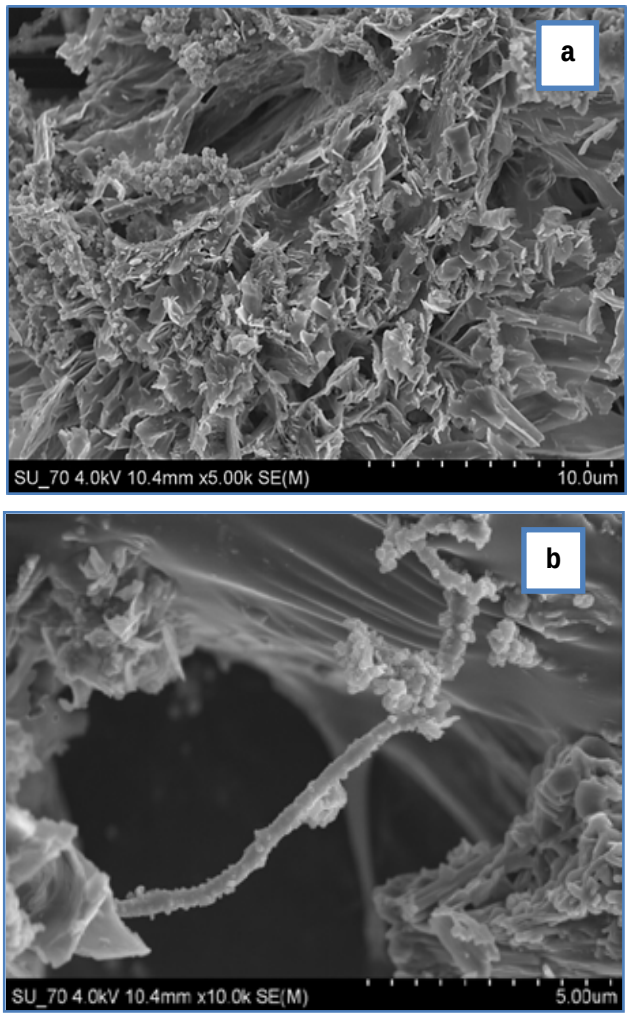

Figure 3. SEM of the C/CPS=25:75 wt. % at 500x (a) and 10 000x (b)

Figure 4 depicts SEM micrographs of C/CPS=75:25 wt. % before immersion in 1.5 SBF for 3 days.

The presented morphology of the prepared sample with a high quality of C is quite different. On the other hand, the CPS ceramic powder is finely distributed on the collagen fibrils on the nanometer level (Fig. 4, a). On the other hand, it is clearly visible the presence of a big spherical particle with diameter ~10 μm. It has a bright colour and the presence of pores which denoting the formation and nucleation of a needle-like HA crystals (Fig. 4, b).

On the base of the presented SEM results and analysis we can conclude that they are in a good agreement with XRD and FTIR on the same samples.

Analysis of the composites after in *vitro test*

The XRD diffraction patterns of the immersed samples with different quantity of C and CPS are given in Fig. 5a and b.

The depicted X-ray diffraction data detects the presence of collagen amorphous halo at ~22° (2θ) and the presence of peaks of HA (PDF 9-0432) after *in vitro* test in 1.5 SBF. From the presented XRD results it is visible that the crystallinity of the immersed samples is lower than that of the samples before immersion (Fig. 1) independently of the quantity of C and CPS powder in them. Obviously, the decrease of the crystallinity could be assigned to the presence of two processes: (i) dissolution of CPS ceramic powders co-existed with the process of supersaturating 1.5 SBF solution and ensuant crystallization of CO_3HA on the surface, and (ii) partial degradation of a C matrix when the composite was placed in SBF solution.

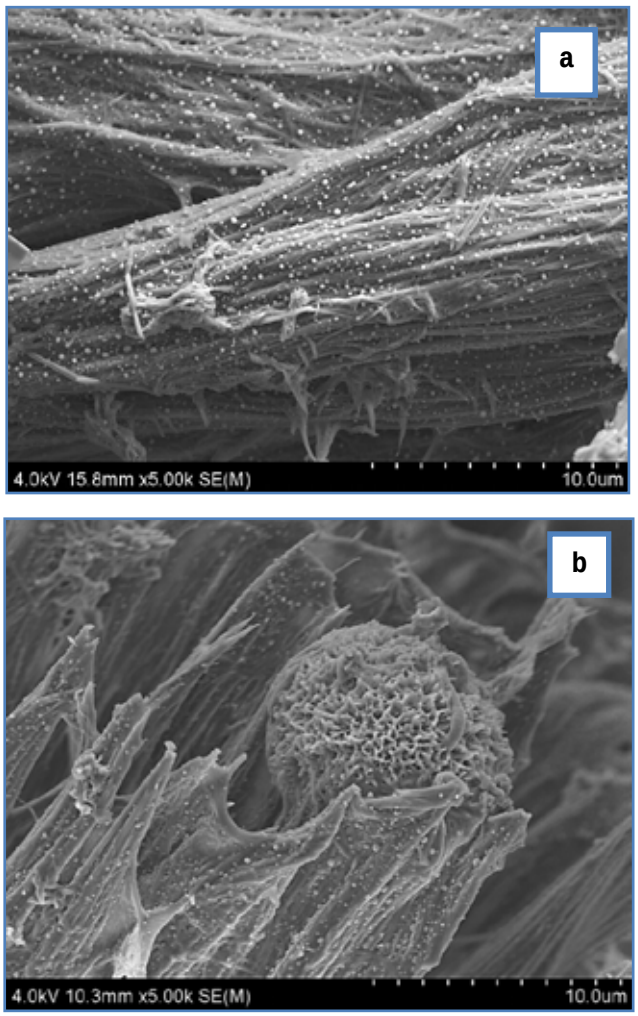

Figure 4. SEM of the C/CPS=75:25 wt. % at 5000x (a) and 5000x (b)

The obtained XRD data clearly proved that C/CPS composites in the presence of ChS are *in vitro* bioactive. On their surface CO_3HA can be formed after in vitro test in 1.5 SBF for 3 days. Compared with our preliminary results on *in vitro* bioactivity of collagen/silicocarnotite composites in the presence of ChS[30], we could make a following conclusion: CPS ceramic powder are most dissolute in 1.5 SBF due to the silicocarnotite. Therefore, the crystallinity of the composites decreased. ChS could not prevent on this process.

The FTIR spectra of the prepared C/CPS composites after immersion in 1.5 SBF for 3 days are given in Fig. 6.

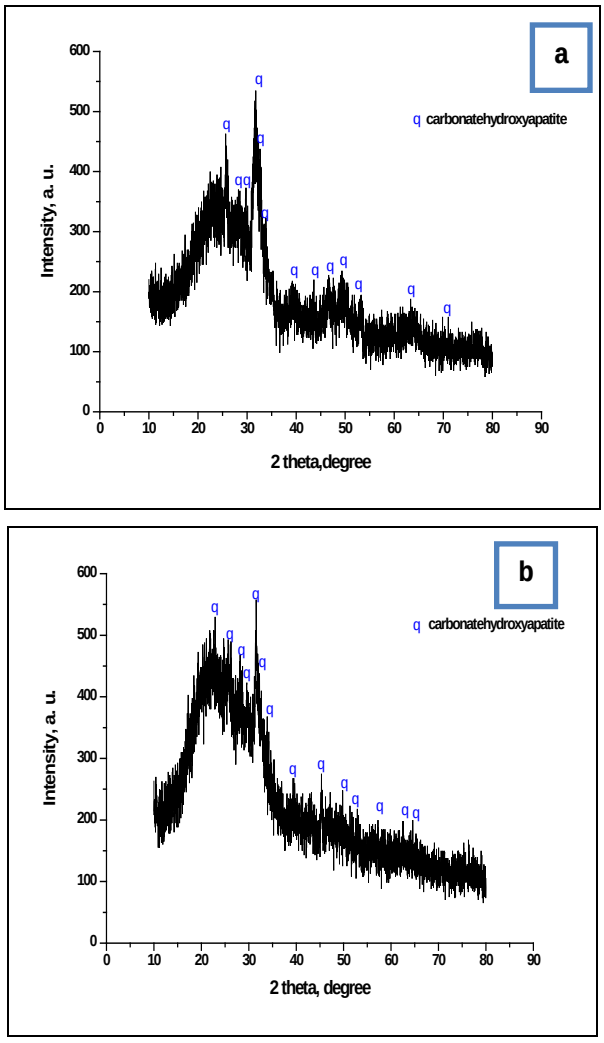

Figure 5. XRD for the C/CPS=25:75 wt. % (a) and C/CPS=75:25 wt. % (b) after soaking in 1.5 SBF for 3 gays

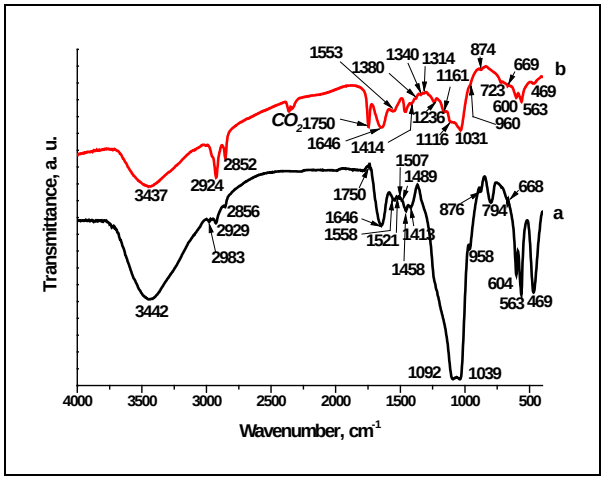

Figure 6. FTIR spectra of the C/CPS=25:75 wt. % (a) and C/CPS=75:25 (b) after in vitro test in 1.5 SBF for 3 days

Figure 6 shows the infra-red absorption bands of CO_3HA which is formed on the surface of the synthesized C/CPS composites after soaking in 1.5SBF for 3 days. For convenience we discussed the phosphate, silicate and carbonate bonds separately.

1.Analysis for the phosphate bands. The very important vibrations of the PO_4^{3-} bands in the FTIR spectra, presented in the Fig. 6, could be distinguished in the three main regions: (i) the peaks with very small intensity, posited at 1039 (1031) cm^{-1} are associated with asymmetric stretch vibration[31]. On the other hand, the presence of these peaks are related with stretching vibrations of PO_4^{3-} in phosphate crystalline phases[32]; (ii) a weak band, centered at 958 (960) cm^{-1} for two composites corresponding to the symmetric stretching[31, 33, 34], and (iii) the well resolved triplet at 604 (600) cm^{-1}, 563 cm^{-1} and 469 cm^{-1} could be assigned to the asymmetric modes[1-3].

2.Analysis for the silicate bands. As can be written elsewhere[35], the most intense spectral future of silicates, appears as a complex group of bands in the range of 1100-900 cm^{-1}, and in the range 550-400 cm^{-1}. On this base, figure 6 clearly shows that the stretching vibrational bands of silicate interfere with phosphate bands. Therefore, the broad peak at around 1039 (1031) cm^{-1} is due to both the ν_1 PO_4^{3-} and the stronger Si-O-Si band [36]. Furthermore, the ν_2 PO_4^{3-} is also masked by the Si-O-Si peak, but the well resolved peaks, posited at 563 cm^{-1} and 604 (600) cm^{-1} is assigned to O-Si-O vibration[35]. The peak with very small intensity, centered at 862 cm^{-1} could be ascribed to the silicone containing HA (Si-HA) structures[35]. The peak, posited at 719 cm^{-1} could be assigned to the presence of small amount of pseudowollastonite (psW) in to the composite[9].

3. Analysis for the carbonate bands. It is known that among the four internal vibrational modes of CO_3^{2-} only two are important for the FTIR analysis – ν_2 and ν_3[37]. In this context the band at 723 cm^{-1} could be assigned to the presence of calcite[38]. The bands at 876 (874) cm^{-1} could be ascribed to the B-type of substitution ($CO_3^{2-} \rightarrow PO_4^{3-}$) in the CO_3HA in the composite samples after soaking. As can be seen from the Fig. 6 the intensity of the CO_3^{2-} band increase as the CPS content increases in the samples. The absorption band at 1380 cm^{-1} (curve b) can be recognized as A-type substitution ($CO_3^{2-} \rightarrow OH^-$) in CO_3HA[39]. The peaks at 1413 (1414) cm^{-1}, 1458 (1458) cm^{-1} and 1521 cm^{-1} indicated the formation of B-type CO_3HA[11].

Analysis for the collagen - as has been written, the band at 1340 cm^{-1}(curve b) in collagen represents not only the COO^-, but a number of bands in the range 1400-1300 cm^{-1}, which are attributed to the presence of type I collagen in biological tissue[13]. This band does not undergo the "red shift" after *in vitro* test in 1.5 SBF for 3 days, i. e. $(COO)_2Ca$ bond does not observe. The band at 1646 cm^{-1} (for the two composites) and at 1558 (1553) cm^{-1} can be assigned to the amide I and amide II from the collagen[12,13]. From the depicted FTIR results are visible that amide I underdoes the "blue shift" from ~1612cm^{-1} (Fig. 2) to 1646 cm^{-1}(Fig. 6). This "blue shift" could be ascribed to the formation of HA on the immersed samples. The same fact is proved for the other polypeptides. For instance, J. Wang et al. denoted that the group vibration of the silk fibroin (SF), HA and SF/HA composite were restrained, because HA crystals nucleated on the nucleation sites of SF[40]. They determined that the amide I band

shifted by 26 cm^{-1} (from 1633 cm^{-1} for pure SF to 1659 cm^{-1} for SF/HA composite), due to the formation of a new coordination band between Ca^{2+} and C-O and N-H groups from SF[40].

SEM images of the soaked in 1.5 SBF solution samples for 3 days, are given in Figure 7.

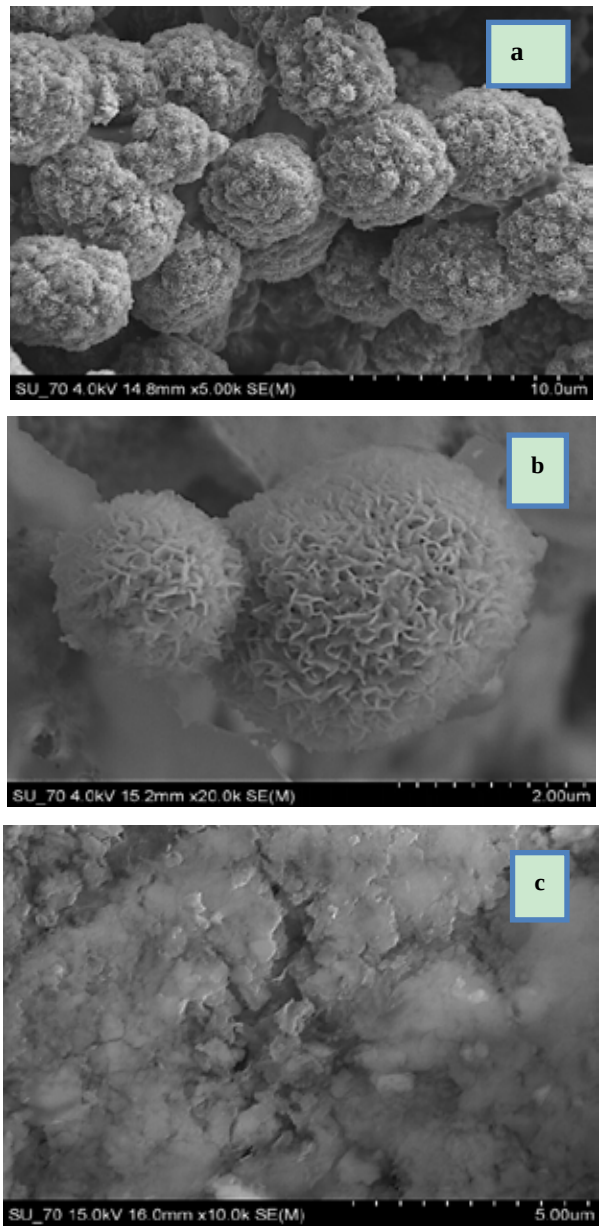

Figure 7. SEM of the C/CPS=75:25 wt. % at 5000x (a), 20 000x (b) and for C/CPS=25:75 wt. % at 10 000x (c) after in vitro test in 1.5 SBF for 3 days in a static condition

SEM images depicts that after 3 days of soaking of the 75:25 wt. % (Fig. 7, a) in 1.5SBF solution in a static condition on their surface HA with spherical morphology are presented. The spherical particles are closed to each other to form aggregates with cauliflower-like assembly. At high magnification view (Fig. 7, b) it is clearly evident that the observed spherical particles have a bright colour and they have some pores denoting the nucleation and formation of HA layer. For the C/CPS=25:75 wt. % composite, SEM image (Fig. 7, c) shows that the surface of the sample fully covered from a new HA layer, but the morphology of the precipitated HA crystals is quite different. As can be seen from this sample we did not observe the presence of aggregated spherical particles with cauliflower-like morphology.

To dissolve this problem we make EDS analysis of the immersed samples.

EDS data are presented in Figure 8.

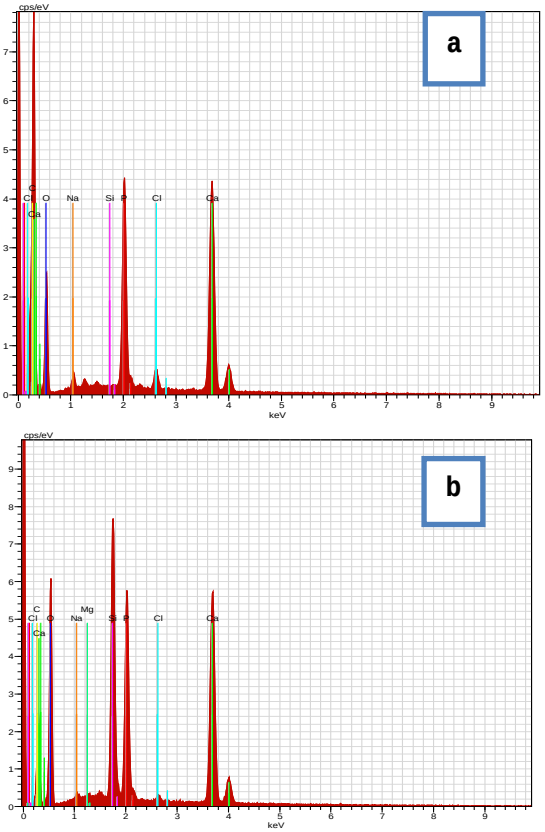

Figure 8. EDS spectra of the C/CPS=75:25 wt. % (a) and C/CPS=25:75 wt. % (b)

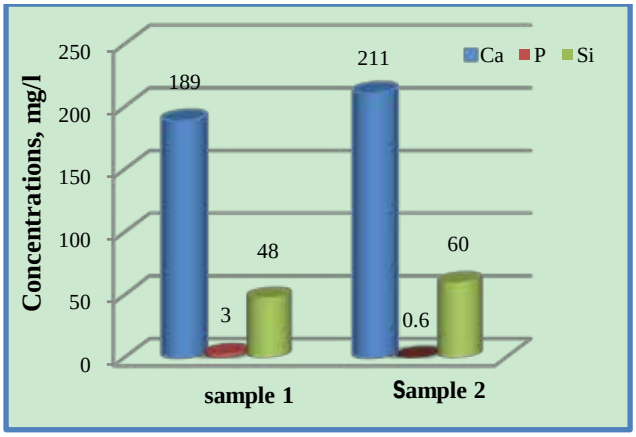

Fugure 9. Changes in Ca, P and Si contents from C/CPS=75:25wt. % (sample 1) and C/CPS=25:75 wt. % (sample 2)

EDS in Fig. 8, a and b showed that both apatites contain primarily Ca and P with Ca/P ratio 1.67 for the C/CPS= 75:25 wt. % (a) and 1.33 for the C/CPS=25:75 wt. % (b). From the calculated Ca/P (at. %) ratio it is evidence that on

the C/CPS=25:75 wt. % the stoichiometric HA is obtained. Contrary, on the C/CPS=25:75 wt. % amorphous calcium phosphate (ACP) was observed[41].

Fugure 9 presents the data for evaluation of the ionic concentration of Ca, P and Si in the 1.5 SBF solutions after immersion of the samples for 3 days by ICP-AES analysis.

From the depicted Fig. 9 it can be seen that the Ca concentration for the samples 1 and 2 slightly increased from 89 mg/l (for 1.5 SBF before soaking) to 189 mg/l (sample 1) and 211 mg/l (sample 2). The quantities of Ca (mg/l) are in accordance with the wt. % ratio of the CPS ceramic powder in the composites. On the other hand, the concentration of P increased from 1 mg/l (for the 1.5 SBF solution) to 3 mg/l (for sample 1) and decreased to 0.6 mg/l (for sample 2). In accordance with XRD data (Fig. 1) and with SEM images of the composite with C/CPS=75:25 wt. % (Fig. 4, a) the high quantity of P for this sample may be explained with the finely dispersed CPS ceramic on the collagen fibrils and with a high dissolution rate of CPS ceramic powder in 1.5 SBF solution. The lower P content in the C/CPS sample with a weight % ratio of the components equal to 25:75 leads us to a conclusion that P may play an active role in a transformation of the sample surface during the immersion in 1.5 SBF solution. Furthermore, from the depicted ICP-AES analysis, we can see that the Si content in 1.5 SBF solutions increased to 48 mg/l (for the sample 1) and to 60 mg/l (for the sample 2). In coincidence with X-ray diffraction data (Fig. 1) we can conclude that the changes in the phase composition (ammonium calcium acetate and $Ca_{15}(PO_4)_2(SiO_4)_6$) after soaking are pronounced for the HA formation. The high quantity of Si in 1.5 SBF solution (sample 2) leads us to infer that Si containing carbonate substituted hydroxyapatite (Si-CO_3HA) may be formed on the immersed C/CPS=25:75 wt. %. For the other sample C/CPS=75:25 wt. % we suppose that Si-CO_3HA also will be formed for longer soaking time.

4. Conclusions

The main purpose of the presented work was to synthesize, characterize and assess the *in vitro* bioactivity of the composites between C and CPS in the presence of ChS. Collagen type I was diluted in 5M CH_3COOH and mixed with CPS powder in a 25:75 and 75:25 wt. % ratio in the presence of ChS. XRD for the samples before *in vitro* test proved that three main phases ammonium calcium acetate, $Ca_{15}(PO_4)_2(SiO_4)_6$ and CO_3HA were observed. FTIR depicted that the chemical interaction between COO^- from ChS and Ca^{2+} from partially dissolved CPS ceramic is proved. β-sheet structures in the collagen might also occur. On the same time Ca-def. HA is formed *in situ* under preparation condition. SEM depicts of the presence of the particles with different morphology. In the C/CPS=75:25 wt. % sample big spherical particles with a bright colour are present, but in the C/CPS=25:75 wt. % some spherical particles are formed on C fibrils. The observation confirmed XRD and FTIR results.

After *in vitro* test in 1.5 SBF for 3 days XRD proved well distinguished HA crystalline phases. On the base of these results we are going closer to the conclusion that the synthesized C/CPS/ChS composites are in vitro bioactive. FTIR analysis determined that the observed "blue shift" for amide I could be assigned to the HA formation on the C/CPS samples. SEM depicts that two kinds of surface particles with different morphology are depicted – big aggregates with cauliflower-like assembly and fully covered surface with quasi-spherical particles. EDS proved the Ca/P ratios 1.67 and 1.33, respectively. On the base of the EDS results we can assume that HA and ACP layers were covered the surface of the synthesized composites. ICP-AES results confirmed XRD, FTIR and SEM results and leads us to conclude that Si-CO_3HA may be formed in the immersed C/CPS composites in the presence of ChS.

REFERENCES

[1] Rhree, S.-H. and Tanaka, J., 2000, Effect of chondroitin sulfate on the crystal growth of hydroxyapatite, J. Am. Ceram. Soc., 83(8), 2100-2102.

[2] Rhree, S.-H., and Tanaka. J., 2001, Synthesis of hydroxyapat ite/collagen/chondroitin sulfate namocomposite by a novel precipitation method, J. Am. Ceram. Soc., 84(2), 459-461.

[3] Rhree, S.-H., and Tanaka, J., 2002, Self-assembly phenomenon of hydroxyapatite nanocrystals on chondroitin sulfate, J. Mater. Sci: Mater. Med., 13, 597-600.

[4] Jiang, H., Liu, X. - Y., Zhang, G., and Li, Y.. 2005, Kinetics and Template Nucleation of self-Assembled Hydroxyapatite Nanocrystallites by Chondroitin Sulfate, The Journal of Biologycal Chemistry, 280(51), 42061-42066.

[5] Xiao, X., He, D., Liu, F., and Liu, R., 2008, Preparation and characterization of hydroxyapatite/chondroitin sulfate composites by biomimetic synthesis, Materials Chemistry and Physics, 112, 838-843.

[6] Gafni, G., Septier, D., and Goldberg M., 1999, Effect of chondroitin sulfate and biglycan on the crystallization af hydroxyapatite under physiological conditions, Journal of Crystal Growth, 205, 618-623.

[7] Rhee, S.-H., Suetsugo, Y., andTanaka, J., 2001, Biomimetic configurational arrays of hydroxyapatite nanocrystals on bio-organs, Biomaterials, 22, 2843-2847.

[8] Chang, M., 2008, Modification of Hydroxyapatite/gelatin Nanocomposite with the addition of Chondroitin Sulfate, Journal of the Korean Cramic Society, 45(10), 573-578.

[9] Radev, L., Hristov, V., Michailova, I., and Samuneva, B., 2009, Sol-gel bioactive glass-ceramics Part I: Calcium Phosphate Silicate/Wollastonite glass-ceramics, Cent. Eur. J. Chem., 7(3), 317-321.

[10] Radev, L., Hristov, V., Michailova, I., and Samuneva, B., 2009, Sol-gel bioactive glass-ceramics Part II: Glass-ceramic s in the CaO-SiO_2-P_2O_5-MgO system, Cent. Eur. J. Chem., 7(3), 322-327.

[11] Radev, L., Hristov, V., Michailova, I., Fernandes, M. H. V.,

and Salvado I. M. M., 2010, In vitro bioactivity of biphasic calcium phosphate silicate glassceramic in CaO-SiO_2-P_2O_5 system, Processing and Application of Ceramics, 4(1), 15-24.

[12] Radev, L., Hristov, V., Samuneva B., and Ivanova, D., 2009, Organic/Inorganic bioactive materials Part II: in vitro bioactivity of Collagen-Calcium Phosphate Silicate/Wollastonite hybrids, Cent. Eur. J. Chem., 7(4), 711-720.

[13] Radev L., Fernandes M.H.V., Salvado I.M., and Kovacheva D., 2009, Organic/Inorganic bioactive materials Part III: in vitro bioactivity of gelatin/silicocarnotite hybrids, Cent. Eur. J. Chem. 7(4) 721-730.

[14] Hristov. V., Radev L., Samuneva B., and Apostolov G., 2009, Organic / inorganic bioactive materials Part I: Synthesis, structure and in vitro assessment of collagen/silicocarnotite biocoatings, Cent. Eur. J. Chem., 7(4), 702-710.

[15] Radev, L., Hristov, V., Fernandes, M. H. V., and Salvado, I. M. M., 2010, Organic/inorganic bioactive materials part IV: In vitro assessment of bioactivity of gelatin-calcium phosphate silicate/wollastonite hybrids, Cent. Eur. J. Chem. 8(2), 278-284.

[16] Radev, L., Hristov, V., Michailova, I., Fernandes, M. H. V., and Salvado, I. M. M., 2011 Collagen/silicocarnotite composites, cross-linked with chondroitin sulphate: in vitro bioactivity, Process. Applic. Ceram., 5(3), 161-170.

[17] Falini, G., Fermani, S., Palazzo, B., and Roveri N., 2008, Helical domain collagen substrates mineralization in simulated body fluid, J. Biomed. Mater. Res., A87(2), 470-478.

[18] Chang, M., and Tanaka, J., 2002, FT-IR study for hydroxyapatite/collagen nanocomposite cross-linked by glutaraldehyde, Biomaterials, 23(24), 4811-4818.

[19] Sachlos, E., Wahl, D., Triffitt J., and Czernuszka J., 2008, The impact of critical point drying with liquid carbon dioxide on collagen–hydroxyapatite composite scaffolds, Acta Biomaterialia, 49(5), 1322-1331.

[20] Alili, D.. (Sweden, 2008) Polypeptide-based nanocomposite materials, Ph.D. Thesis, Linkoping University, Instititute of Technology.

[21] Liard, D., Mulvihill, M., and Lillig, J., 2008 Membrane-induced peptide structural changes monitored by infrared and circular dichroism spectroscopy, Biophys. J., 145, 72-78.

[22] Petibois, C., Gouspillou, G., Wehbe K., Delage, J.-P., and Déléris, G., 2011, Analysis of type I and IV collagens by FT-IR spectroscopy and imaging for a molecular investigation of skeletal muscle connective tissue, Anal. Bioanal. Chem., 400, 1961-1966.

[23] Musumeci, A., Frost R., and Waclawik E., 2007, A spectroscopic study of the mineral paceite (calcium acetate), Specrochimica Acta Part A, 67, 649-661.

[24] Zhang, H., and Zhang, M., 2011, Characterization and thermal behaviour of calcium deficient hydroxyapatite whiskers with varios Ca/P ratios, Materials Chemistry and Physics, 128, 642-648.

[25] Tamai, M., Nakamura, M., Issiki, T., Nishio, K., Endoh, H., and Nakahira, A., 2003, A metastable phase in thermal decomposition of Ca-deficient hydroxyapatite, J. Mater. Sci.: Mater. Med., 14, 617-622.

[26] Baxter, J., Biltz, R., and Pellegrino, E., 1966, The physical state of bone carbonate:a comparative infra-red study in several mineralized tissues, Yale Jornal of Biology and Medicine, 38, 456-470.

[27] Awonusi, A., Morris M., and Tecklenburg, M., 2007, Carbonate Assignment and Calibration in the Raman Spectrum of Apatite, Calcified Tissue International, 81(1), 46-52.

[28] Thian, E.S., Huang, J., Vickers, M., Best, S., Barber, Z., and Bonfield, W., 2006, Silicon-substituted hydroxyapatite (SiHA): A novel calcium phosphate coating for biomedical applications, J. Mater. Sci., 41, 709-714.

[29] Zou, Sh., Huang, J., Best, S., and Bonfield, W., 2005, Crystal imperfection studies of pure and silicon substituted hydroxyapatite using Raman and XRD, J. Mater. Sci.: Mater. Med., 16, 1143-1148.

[30] Radev, L., Hristov. V., Michailova, I., Fernandes, M. H. V., and Salvado, I. M. M., 2011, Collagen/silicocarnotite composites, cross-linked with chondroitin sulphate: in vitro bioactivity, Processing and Application of Ceramics, 5(3), 161-170.

[31] Federman, S.R., Costa, V.C., Vasconcelos, D.C., and Vasconcelos, W.L., 2007, Sol-gel SiO_2-CaO-P_2O_5 biofilm with surface engineered for medical application, Mater. Res., 10, 177-181.

[32] Luna-Zaragoza, D., Romero-Guzmán, E. T., and Reyes-Gutiérrez. L. R., 2009, Surface and Physicochemical Charac terization of Phosphates Vivianite, $Fe_2(PO_4)_3$ and Hydroxyapatite, $Ca_5(PO_4)_3OH$, Journal of Minerals & Materials Characterization & Engineering, 8(8), 591-609.

[33] Patel, N., Best, S., Bonfield, W., Gibson, I., Hing, K., Damien, E. and Revell, P., 2002, A comparative study on the in vitro behaviour of hydroxyapatite and silicon substituted hydroxyapatite granules, J. Mater. Sci.: Mater. Med., 13, 1199-1208.

[34] Salma, K., Berzina-Cimdina, L., and Borodajenko, N., 2010, Calcium phosphate bioceramics prepared from wet chemically precipitated powders, Process. Applic. Ceram., 4 (1), 45-51.

[35] Mostafa, N. Y., Hassan, H. M., and Elkader, O., 2011, Preparation and Characterization of Na^+, SiO_4^{4-}, and CO_3^{2-} Co-Substituted Hydroxyapatite, J. Am. Ceram. Soc., 94 (5), 1584-1590.

[36] Xu, G., Aksay, I. A., and Groves, J.T., 2001, Continuous crystalline carbonate apatite thin films. A biomimetic approach, J. Am. Chem. Soc., 123, 2196-2203.

[37] Leventouri, Th., Antonakos, A., Kyriacou, A., Venturelli, R., Liarokapis, E., and Perdikatsis, V. 2009, Crystal structure studies of human dental apatite as a function of age, Int. J. Biomater., 2009, 1-6.

[38] Tomić, Z., Makreski, P., and Gajić, B., 2010, Identification and spectra-structure determination of soil minerals: Raman study supported by IR spectroscopy and X-ray powder diffraction, J. Raman Spectroscopy, 41(5), 582-586.

[39] Doi, Y., Moriwaki, Y., Aoba, T., Takahashi, J., and Joshin, K.,

1982, ESR and IR studies of Carbonate Containing Hydroxyapatites, Calcified Tissue International, 34, 178-181.

[40] Wang, J., Yu, F., Qu, L., Meng, X., and Wen, S. G., 2010, Study of synthesis of nano-hydroxyapatite using a silk fibroin template, Biomed. Mater., 5, 1-6.

[41] Dorozhkin, S. V., 2009, Calcium Orthophosphate Cements and Concretes, Materials, 221-291.